

Quadratic response theory for the interaction of charged particles with an electron gas

J. M. Pitarke and I. Campillo

*Materia Kondentsatuaren Fisika Saila, Zientzi Falkultatea, Euskal Herriko Unibertsitatea,
644 Posta kutxatila, 48080 Bilbo, Basque Country, Spain*

(February 1, 2008)

Abstract

A survey is presented of the theoretical status of quadratic response theories for the understanding of nonlinear aspects in the interaction of charged particles with matter. In the frame of the many-body perturbation theory we study the interaction of charged particles with the electron gas, within the random-phase approximation (RPA). In particular, nonlinear corrections to the stopping power of an electron gas for ions are analyzed, and special emphasis is made on the contribution to the stopping power coming from the excitation of single and double plasmons. Double plasmon mean free paths of swift electrons passing through an electron gas are also discussed.

29.70.Gn,34.50.Bw,61.80.Mk

I. INTRODUCTION

A quantitative description of the interaction of charged particles with matter is of basic importance in many different theoretical and applied areas¹. When an ion penetrates condensed matter it causes changes in the charge state of the ion, electrons may be stripped from the ion or captured from electronic states of the solid, dynamic screening by valence electrons originates a wake of electron density fluctuations, and the ion may lose energy to the medium through different types of elastic and inelastic collision processes. When a swift electron travels in a solid it may also lose energy to the medium. While at relativistic velocities radiative losses may become important, for incident charged particles in the non-relativistic regime the significant energy losses appear as a consequence of electron-electron interactions giving rise to the generation of electron-hole pairs, collective oscillations, and inner-shell excitations and ionizations.

Since the pioneering works of Bohm and Pines² the response of conduction electrons in metals to external charged particles has been represented within the electron gas model, by replacing the ionic lattice by a homogeneous background which serves to provide neutrality to the system. The screening properties of a system of interacting electrons are determined, within linear response theory, by the wavevector and frequency dependent longitudinal dielectric function $\epsilon_{\mathbf{q},\omega}$. In the self-consistent field, or random-phase, approximation, the dielectric function of an electron gas was first derived by Lindhard³, and, subsequently, a number of workers have given alternative expressions for $\epsilon_{\mathbf{q},\omega}$, incorporating various many-body higher order local-field corrections^{4,5} and band effects^{6,7}. The effect of dissipative processes occurring in a real metal and conversion of plasmons into multiple electron-hole pairs may be allowed for in an approximate way by including a damping coefficient in the dielectric function⁸.

Nevertheless, the validity of linear response theory, which treats the perturbing potential to lowest order, is not obvious a priori. Although lowest-order perturbation theory leads to energy losses that are proportional to the square of the projectile charge⁹, Z_1e , from

measurements on positive and negative pions¹⁰ and, also, on protons and antiprotons¹¹ it is known that the energy loss exhibits a dependence on the sign of the charge^{12–14}. On the other hand, experimentally observed nonlinear double plasmon excitations^{15,16} cannot be described within linear response theory^{17,18}, and nonlinearities may also play an important role on the electronic wake generated by moving ions in an electron gas^{20,21}. Finally, lowest order perturbation theory breaks down when the projectile is capable of carrying bound electrons with it¹.

The first full nonlinear calculation of the electronic stopping power of an electron gas was performed by Echenique et al²², in the low-velocity limit. They used a scattering theory approach to the stopping power and the scattering cross sections were calculated for a statically screened potential which was determined self-consistently by using density-functional theory. These static screening calculations have recently been extended to velocities approaching the Fermi velocity²³. Alternatively, in the case of incident ions a theoretical effective charge can be associated²⁴, and nonlinearities can be investigated, within quadratic response theory, extending, therefore, the range of linear response theory and providing results for arbitrary velocity. A quadratic response theory of the energy loss of charged particles in an electron gas has recently been carried out²⁵, by following a diagrammatic analysis of many-body interactions between a moving charge and the electron gas.

In this paper we present a survey of the theoretical status of investigations carried out within quadratic response theory for the understanding of nonlinear aspects in the interaction of charged particles with an electron gas. We present general procedures to calculate, within many-body perturbation theory, double plasmon excitation probabilities, Z_1^3 contributions to the stopping power of an electron gas for ions and the nonlinear wake potential generated by moving ions in an electron gas. We focus on the contribution to the stopping power coming from the excitation of single and double plasmons.

Unless otherwise is stated, atomic units are used throughout ($\hbar = m_e = e^2 = 1$).

II. THEORY

We consider a probe of charge Z_1 interacting with a many-particle system. The excitation of eigenmodes of the target together with the reaction of the probe to these excitations can be described by the self-energy of the probe. For an incoming particle in a state ϕ_0 of energy p^0 one writes²⁶:

$$\Sigma_0 = \int d^3\mathbf{r} \int d^3\mathbf{r}' \phi_0^*(\mathbf{r}) \Sigma(\mathbf{r}, \mathbf{r}', p^0) \phi_0(\mathbf{r}'), \quad (2.1)$$

where $\Sigma(\mathbf{r}, \mathbf{r}', p^0)$ represents the non-local self-energy.

The real part of Σ_0 gives us the real energy shift due to the interaction with the medium, and the imaginary part is well-known to be directly related to the damping rate experienced by the particle as a consequence of the interaction with real excitations of the target:

$$\gamma = -2\text{Im}\Sigma_0. \quad (2.2)$$

We take the target to be described by an isotropic homogeneous assembly of electrons immersed in a uniform background of positive charge and volume Ω , and we use, therefore, plane waves to describe the incident particle states. Consequently,

$$\gamma = -2\text{Im}\Sigma_p, \quad (2.3)$$

where Σ_p represents the Fourier transform of $\Sigma(\mathbf{r}, \mathbf{r}', p^0)$, $p = (\mathbf{p}, p^0)$, and \mathbf{p} is the momentum of the probe.

The self-energy, Σ_p , can be calculated in the so-called GW approximation^{27,28}:

$$\Sigma_p = iZ_1^2 \int \frac{d^4q}{(2\pi)^4} G_{p-q} W_q, \quad (2.4)$$

where G_k and W_q represent Fourier transforms of the Green function for the probe and the time-ordered screened interaction, respectively. In applying this formula we replace G_k by the zero order approximation; for electrons ($Z_1 = -1$)²⁹:

$$G_k^0 = \frac{1 - n_{\mathbf{k}}}{k^0 - \omega_{\mathbf{k}} + i\eta} + \frac{n_{\mathbf{k}}}{k^0 - \omega_{\mathbf{k}} - i\eta}, \quad (2.5)$$

where $\omega_{\mathbf{k}} = \mathbf{k}^2/2$, η is a positive infinitesimal, and $n_{\mathbf{k}}$ represents the occupation number, which at a temperature of $T = 0K$ is

$$n_{\mathbf{k}} = \theta(k_F - |\mathbf{k}|), \quad (2.6)$$

k_F being the Fermi momentum and $\theta(x)$, the Heaviside function.

The dynamically screened interaction, W_q , can be represented as follows:

$$W_q = \epsilon_q^{-1} v_{\mathbf{q}}, \quad (2.7)$$

where $v_{\mathbf{q}}$ represents the Fourier transform of the bare Coulomb interaction:

$$v_{\mathbf{q}} = \frac{4\pi e^2}{\mathbf{q}^2}, \quad (2.8)$$

and ϵ_q is the dielectric function, which is related to the density-density response function, χ_q , by:

$$\epsilon_q^{-1} = 1 + v_{\mathbf{q}} \chi_q. \quad (2.9)$$

Now, introduction of Eqs. (2.5) and (2.7) into Eq. (2.4), and Eq. (2.4) into Eq. (2.3) gives the following result for the damping rate of incident electrons with energy above the Fermi level:

$$\gamma = \sum_{\mathbf{q}} \int_0^\infty \frac{dq^0}{2\pi} P_q, \quad (2.10)$$

where P_q represents the probability of transferring four-momentum $q = (\mathbf{q}, q^0)$ to the electron gas:

$$P_q = -\frac{4\pi}{\Omega} Z_1^2 \text{Im} W_q \delta(q^0 - p^0 + \omega_{\mathbf{p}-\mathbf{q}}) \theta(\omega_{\mathbf{p}-\mathbf{q}} - E_F). \quad (2.11)$$

The delta function in this expression appears as a consequence of energy conservation, and the step function, $\theta(\omega_{\mathbf{p}-\mathbf{q}} - E_F)$, ensures that no electrons lose enough energy to fall below the Fermi level.

When the probe is not an electron the occupation number of Eq. (2.6) is zero, i.e., we need not take account of the fact that the incident electron cannot make transitions to occupied states in the Fermi sea:

$$P_q = -\frac{4\pi}{\Omega} Z_1^2 \text{Im} W_q \delta(q^0 - p^0 + \omega_{\mathbf{p}-\mathbf{q}}), \quad (2.12)$$

and if the probe has mass $M \gg 1$, then recoil can be neglected in the argument of the delta function to give:

$$P_q = -\frac{4\pi}{\Omega} Z_1^2 \text{Im} W_q \delta(q^0 - \mathbf{q} \cdot \mathbf{v}), \quad (2.13)$$

where \mathbf{v} represents the velocity of the incoming particle.

The inverse mean free path of the probe is easily obtained as follows:

$$\lambda^{-1} = \frac{1}{v} \sum_{\mathbf{q}} \int_0^\infty \frac{dq^0}{2\pi} P_q, \quad (2.14)$$

and the stopping power of the target for the probe is obtained as the energy loss per unit path length of the projectile, after multiplying the probability P_q by the energy transfer q^0 :

$$-\frac{dE}{dx} = \frac{1}{v} \sum_{\mathbf{q}} \int_0^\infty \frac{dq^0}{2\pi} q^0 P_q. \quad (2.15)$$

In the so-called time-dependent Hartree, or random-phase, approximation the exact linear response function to a screened charge is replaced by the response function of the non-interacting electron gas:

$$\chi_q^0 = -2i \int \frac{d^4 k}{(2\pi)^4} G_k^0 G_{k+q}^0, \quad (2.16)$$

thus replacing the linear response function to an external charge, χ_q , by

$$\chi_q^{RPA} = \chi_q^0 + \chi_q^0 v_{\mathbf{q}} \chi_q^{RPA}. \quad (2.17)$$

Within this approximation the self-energy of Eq. (2.4) can be represented diagrammatically as in Fig. 1, and cutting the diagrams of this figure through the two-electron lines

in all the bubbles would lead to the open diagrammatic representation of scattering amplitudes shown in Ref. 25. In particular, if $M \gg 1$ the incident particle can be treated as a prescribed source of energy and momentum and one finds²⁵:

$$S_{f,i} = \frac{2\pi i}{\Omega} Z_1 \int d^4q \delta^4(q + s - p) W_q^{RPA} \delta(q^0 - \mathbf{q} \cdot \mathbf{v}), \quad (2.18)$$

where $s = (\mathbf{s}, s^0)$, $p = (\mathbf{p}, p^0)$, and W_q^{RPA} represents the random-phase approximation to the screened interaction of Eq. (2.7).

Then, the probability of transferring four-momentum q to a free-electron gas by moving a particle from inside the Fermi sea ($|\mathbf{s}| < q_F$) to outside ($|\mathbf{p}| > q_F$), thus creating an electron-hole pair, is derived from the square of the matrix element $S_{f,i}$:

$$P_q = 2 \sum_{\mathbf{s}} n_{\mathbf{s}} \sum_{\mathbf{p}} (1 - n_{\mathbf{p}}) |S_{fi}|^2 \delta_{q,p-s}^4, \quad (2.19)$$

where $\delta_{q,q'}^4$ is the symmetric Kronecker δ symbol, and introduction of Eq. (2.18) into Eq. (2.19) gives exactly the result of Eq. (2.13) found by the self-energy method.

It is obvious at this point that double plasmon excitations cannot be described within the GW-RPA approximation to the self-energy, represented diagrammatically in Fig. 1; double excitations can only be described, within the GW approximation, with inclusion in the screened interaction of dynamic local-field corrections. On the other hand, the study of Z_1^3 effects in the stopping power of an electron gas for ions and, also, the study of nonlinearities in the wake generated by moving ions in an electron gas require going beyond the so-called GW approximation. The main ingredient in the investigation of both double plasmon excitations and Z_1^3 effects is the symmetrized quadratic response function of the non-interacting electron gas:

$$M_{q,q_1} = i \int \frac{d^4k}{(2\pi)^4} G_k^0 G_{k+q}^0 \left[G_{k+q_1}^0 + G_{k+q-q_1}^0 \right], \quad (2.20)$$

which gives account of the quadratic response of the system to a given charge. The real part of this three-point function was first evaluated by Cenni et al³⁰, explicit expressions for the imaginary part in terms of a sum over hole and particle states have been presented recently^{14,25}, and an extension to imaginary frequencies has also been given³¹.

A. Double excitation probabilities

Treating the probe as an external source of energy and momentum, the matrix element corresponding to the process of carrying the system from an initial state $a_{i_1}^+ a_{i_2}^+ |\Phi_0\rangle$ to a final state $a_{f_1}^+ a_{f_2}^+ |\Phi_0\rangle$ is

$$S_{f_1 f_2, i_1 i_2} = \frac{\langle \Phi_0 | a_{f_1} a_{f_2} S a_{i_1}^+ a_{i_2}^+ | \Phi_0 \rangle}{\langle \Phi_0 | S | \Phi_0 \rangle}, \quad (2.21)$$

where Φ_0 is the vacuum state, a_i and a_i^+ are annihilation and creation operators for fermions, respectively, and S is the scattering matrix. S is obtained as a time-ordered exponential in terms of the perturbing Hamiltonian and field operators $\Psi(x)$ and $\Psi^+(x)$ destroying and creating, respectively, a particle at the point \mathbf{r} at the time t .

Now, one can apply Wick's theorem, we note that only normal ordered products with four uncontracted field operators contribute, and we find, up to second order in the probe charge a result that can be represented diagrammatically as in Fig. 2. Within the random-phase approximation, the screened interaction, W_q , is obtained from Eqs. (2.7), (2.9) and (2.17), and, accordingly, all self-energy and vertex insertions have been neglected. On the other hand, exchange processes and, also, ladder contributions have not been introduced into Eq. (2.21), since they all lead to scattering probabilities that are of a higher order in the screened interaction.

Finally, the probability for transferring four-momentum q to a free-electron gas by moving two particles from inside the Fermi sea ($|\mathbf{s}_1| < q_F$ and $|\mathbf{s}_2| < q_F$) to outside ($|\mathbf{p}_1| < q_F$ and $|\mathbf{p}_2| < q_F$) is derived from the square of the matrix element $S_{f_1 f_2, i_1 i_2}$:

$$P_q = 4 \sum_{q_1} \sum_{\mathbf{s}_1} n_{\mathbf{s}_1} \sum_{\mathbf{s}_2} n_{\mathbf{s}_2} \sum_{\mathbf{p}_1} (1 - n_{\mathbf{p}_1}) \sum_{\mathbf{p}_2} (1 - n_{\mathbf{p}_2}) |S_{f_1 f_2, i_1 i_2}|^2 \delta_{q_1, p_1 - s_1}^4 \delta_{q - q_1, p_2 - s_2}^4. \quad (2.22)$$

If the probe were not a heavy particle, then recoil should be introduced into the argument of the delta function to ensure energy conservation, and, in particular, if the probe were an electron a step function should also be introduced to ensure that the probe does not lose enough energy to fall below the Fermi level. Then the contribution of Eq. (2.22)

to the probability that is proportional to Z_1^2 , obtained after introduction of the matrix element $S_{f_1 f_2, i_1 i_2}$ represented diagrammatically in Fig. 2 into Eq. (2.22), would coincide with contributions derived from a GW approximation to the self-energy with inclusion, in the screened interaction, of corresponding dynamic local-field corrections.

In particular, the only Z_1^2 contribution to the probability of Eq. (2.22) which might represent the real excitation of a double plasmon comes from the square of the scattering amplitude represented by the second diagram of Fig. 2. It is given by the following expression:

$$P_q = \frac{16\pi}{\Omega^2} Z_1^2 W_q^{-2} \sum_{\mathbf{q}_1} \int_0^{q^0} \frac{dq_1^0}{2\pi} \text{Im} W_{q_1} \text{Im} W_{q-q_1} |M_{q, q_1}|^2 \delta(q^0 - p^0 + \omega_{\mathbf{p}-\mathbf{q}}) \theta(\omega_{\mathbf{p}-\mathbf{q}} - E_F). \quad (2.23)$$

Introduction of this probability into Eq. (2.14) gives, after approximating the linear and quadratic response functions by their low- q limits, the following high-velocity limit for the Z_1^2 contribution to the inverse mean free path coming from the excitation of a double plasmon¹⁸:

$$\lambda_{2p}^{-1} \approx 0.164 \frac{\sqrt{r_s}}{36\pi v^2}. \quad (2.24)$$

Numerical study shows¹⁹ that introduction of the full RPA response functions gives a result for λ_{2p}^{-1} which has, in the high-velocity limit, the same dependence on v as the approximation of Eq. (2.24), though it is, for $r_s = 2.07$, larger than this approximation by a factor of 2.16.

B. Z_1^3 correction to the stopping power for ions

The stopping power of an electron gas for a probe of charge Z_1 , mass $M \gg 1$ and velocity \mathbf{v} is obtained after introduction of the probability P_q into Eq. (2.15). Up to third order in the projectile charge:

$$-\frac{dE}{dx} = \frac{1}{v} \sum_{\mathbf{q}} \int_0^\infty \frac{dq^0}{2\pi} q^0 (P_q^{\text{single}} + P_q^{\text{double}}), \quad (2.25)$$

where P_q^{single} and P_q^{double} , probabilities of transferring four-momentum q to the electron gas by creating single and double excitations, respectively, are obtained from Eqs. (2.19) and (2.22), respectively. There,

$$S_{f,i} = \frac{2\pi}{\Omega} Z_1 \int d^4 q \delta^4(q + s - p) \delta(q^0 - \mathbf{q} \cdot \mathbf{v}) \\ \times \left\{ W_q + 2\pi Z_1 \left[iW_{q_1} W_{q-q_1} G_{s+q}^0 + -iW_q W_{q_1} W_{q-q_1} M_{q,q_1} \right] \delta(q_1^0 - \mathbf{q}_1 \cdot \mathbf{v}) \right\}, \quad (2.26)$$

which is represented diagrammatically in Fig. 3, and

$$S_{f_1 f_2, i_1 i_2} = \frac{2\pi i}{\hbar^2 \Omega^2} Z_1 \int d^4 q_1 \delta^4(q_1 + s_1 - p_1) \int d^4 q \delta^4(q - q_1 + s_2 - p_2) \delta(q^0 - \mathbf{q} \cdot \mathbf{v}) \\ \times \left\{ \left[W_q W_{q-q_1} \left(G_{s+q}^0 + G_{s-q+q_1}^0 \right) - W_q W_{q_1} W_{q-q_1} M_{q,q_1} \right] + 2\pi i Z_1 W_{q_1} W_{q-q_1} \delta(q_1^0 - \mathbf{q}_1 \cdot \mathbf{v}) \right\}, \quad (2.27)$$

represented diagrammatically in Fig. 2. Processes involving higher-order excitations have not been included.

Now, after introduction of Eqs. (2.26) and (2.27) into Eqs. (2.19) and (2.22), respectively, we find, up to third order in the ion charge:

$$-\frac{dE}{dx} = (-dE/dx)^{\text{single}_1} + (-dE/dx)^{\text{single}_2} + (-dE/dx)^{\text{double}_2}, \quad (2.28)$$

where $(-dE/dx)^{\text{single}_1}$ represents the Z_1^2 contribution to the stopping power coming from single excitations:

$$(-dE/dx)^{\text{single}_1} = -\frac{2}{v} Z_1^2 \int \frac{d^3 \mathbf{q}}{(2\pi)^3} \int_0^\infty dq^0 q^0 \text{Im} W_q \delta(q^0 - \mathbf{q} \cdot \mathbf{v}), \quad (2.29)$$

and $(-dE/dx)^{\text{single}_2}$ and $(-dE/dx)^{\text{double}_2}$ represent Z_1^3 contributions to the stopping power coming from single and double excitations, respectively:

$$(-dE/dx)^{\text{single}_2} = -\frac{4}{v} Z_1^3 \int \frac{d^3 \mathbf{q}}{(2\pi)^3} \int_0^\infty dq^0 q^0 \delta(q^0 - \mathbf{q} \cdot \mathbf{v}) \int \frac{d^3 \mathbf{q}_1}{(2\pi)^3} \int_{-\infty}^\infty dq_1^0 \delta(q_1^0 - \mathbf{q}_1 \cdot \mathbf{v}) \\ \times \left[\text{Im} W_q \text{Re} (W_{q_1} W_{q-q_1} M_{q,q_1}) + \text{Re} (W_q^* W_{q_1} W_{q-q_1}) H_{q,q_1} \right] \quad (2.30)$$

and

$$(-dE/dx)^{\text{double}_2} = -\frac{8}{v} Z_1^3 \int \frac{d^3 \mathbf{q}}{(2\pi)^3} \int_0^\infty dq^0 q^0 \delta(q^0 - \mathbf{q} \cdot \mathbf{v}) \int \frac{d^3 \mathbf{q}_1}{(2\pi)^3} \int_0^{q^0} dq_1^0 \delta(q_1^0 - \mathbf{q}_1 \cdot \mathbf{v}) \\ \times \left[\text{Im} W_{q_1} \text{Im} W_{q-q_1} \text{Im} (W_q M_{q,q_1}) + \text{Im} (W_q W_{q_1}^*) \text{Im} W_{q-q_1} (H_{q_1,q} + H_{q_1,-(q-q_1)}) \right], \quad (2.31)$$

with

$$H_{q,q_1} = 8\pi^4 P \int \frac{d^3\mathbf{s}}{(2\pi)^3} n_{\mathbf{s}} \int \frac{d^3\mathbf{p}}{(2\pi)^3} (1 - n_{\mathbf{p}}) \delta^3(\mathbf{q} - \mathbf{p} + \mathbf{s}) \\ \times \left[\frac{\delta(q^0 + \omega_{\mathbf{s}} - \omega_{\mathbf{p}})}{q_1^0 + \omega_{\mathbf{s}} - \omega_{\mathbf{s}+\mathbf{q}_1}} + \frac{\delta(q^0 - \omega_{\mathbf{s}} + \omega_{\mathbf{p}})}{-(q^0 - q_1^0) + \omega_{\mathbf{s}} - \omega_{\mathbf{s}+\mathbf{q}-\mathbf{q}_1}} \right] + (q_1 \rightarrow q - q_1), \quad (2.32)$$

which is related to the imaginary part of the three-point function of Eq. (2.20) by^{14,25}:

$$\text{Im}M_{q,q_1} = H_{q,q_1} + H_{q_1,q} + H_{(q-q_1),-q_1}. \quad (2.33)$$

The contribution to the Z_1^2 stopping power coming from double excitations, which is of higher order in the screened interaction than the contribution of Eq. (2.29), has not been included in Eq. (2.28). However, contributions of Eqs. (2.30) and (2.31), which are proportional to Z_1^3 , are all of the same order in the screened interaction, they all need, therefore, to be taken into account, and they all can be derived from the knowledge of the Z_1^3 contribution to the self-energy by going beyond the GW approximation.

It is interesting to notice that Z_1^3 contributions to the stopping power that are proportional to the product of two imaginary parts of the screened interaction, appearing as a consequence of both single and double excitations, can be combined, and we, also, find that contributions to the Z_1^3 stopping power that are proportional to the product of three imaginary parts of the screened interaction, coming from single and double excitations, cancel out.

Consequently, one finds the following result for the contribution to the stopping power that is proportional to Z_1^3 :

$$(-dE/dx)^{(2)} = (-dE/dx)^{\text{single}_2} + (-dE/dx)^{\text{double}_2} = \\ -\frac{4}{v} Z_1^3 \int \frac{d^3\mathbf{q}}{(2\pi)^3} \int_0^\infty dq^0 q^0 \delta(q^0 - \mathbf{q} \cdot \mathbf{v}) \int \frac{d^3\mathbf{q}_1}{(2\pi)^3} \int_{-\infty}^\infty dq_1^0 \delta(q_1^0 - \mathbf{q}_1 \cdot \mathbf{v}) \\ \times [f_1(q, q_1) + f_2(q, q_2) + f_3(q, q_1)] \quad (2.34)$$

where

$$f_1(q, q_1) = \text{Im}W_q \text{Re}W_{q_1} \text{Re}W_{q-q_1} \text{Re}M_{q,q_1}, \quad (2.35)$$

$$f_2(q, q_1) = \text{Re}W_q \text{Re}W_{q_1} \text{Re}W_{q-q_1} H_{q,q_1}, \quad (2.36)$$

and

$$f_3(q, q_1) = -2\text{Im}W_q \text{Im}W_{q_1} \text{Re}W_{q-q_1} H_{q_1, q}. \quad (2.37)$$

Contributions to the Z_1^3 stopping power of Eq. (2.34) coming from f_1 and f_2 of Eqs. (2.35) and (2.36) both appear as a consequence of single excitations: the first one comes from the cross product between the first and third diagrams of Fig. 3, and gives, therefore, the contribution from losses to one-step single excitations generated by the quadratically screened ion potential, while the second term comes from the cross product between the first and second diagrams of Fig. 3 and gives the contribution from losses to two-step single excitations generated by the linearly screened ion potential. The third term comes from both cross products, and, also, from losses to double excitations. Contributions coming from single plasmons are included in both f_1 and f_3 , and contributions coming from the excitation of double plasmons are only included in f_3 .

Alternatively, the stopping power of an electron gas can be obtained from the knowledge of the wake potential induced in the vicinity of the projectile, as the induced retarding force that the polarization charge distribution exerts on the projectile itself, and a second-order many body perturbation analysis of the wake potential²¹ at \mathbf{r} , defined as the mean value of the interaction between a test unit positive charge at that point and the electron gas, leads to Eq. (2.34) for the Z_1^3 stopping power, as demonstrated in Ref. 25.

For high velocities of the probe the electron gas can be considered as if it were at rest, one can use, therefore, the so-called static electron gas approximation for both linear and quadratic response functions, and this results in f_2 and f_3 giving no contribution to the integral of Eq. (2.34), i.e., in the high-velocity limit only the contribution to the Z_1^3 stopping power that is proportional to only-one imaginary part of the linearly screened interaction, W_q , is different from zero. Furthermore, it has been shown²⁵ that this contribution to the Z_1^3 effect can be approximated, in the high-velocity limit, by :

$$(-dE/dx)^{(2)} = Z_1^3 \frac{\omega_p^2}{v^2} L_1, \quad (2.38)$$

where ω_p represents the plasma frequency $\omega_p^2 = 4\pi n$, n being the electron density of the medium, and L_1 is the Z_1^3 correction to the so-called stopping number:

$$L_1 \approx 1.42 \frac{\pi \omega_p}{v^3} \ln \frac{2v^2}{2.13\omega_p}. \quad (2.39)$$

At high velocities both the wake potential and the stopping power can also be derived within a quantum hydrodynamical model of the electron gas. In this model, we expand the nonlinear hydrodynamical equations and find, after quantization, a result for the Hamiltonian of the electron plasma-heavy ion system, in terms of the triple vertex interaction between three excitations, that exactly agrees with the result obtained by Ashley and Ritchie¹⁷ by following a different procedure. Then, we find second and third order wake potentials and electronic stopping powers, and, also, double plasmon excitation probabilities that coincide with plasmon-pole like approximations to the full RPA results³².

III. RESULTS

Contributions to electron inelastic mean free paths coming from single excitations of the electron plasma have been calculated in the high velocity limit², and, also, in the full RPA³³. Fig. 4 shows, as a solid line, our full RPA results for the double plasmon inverse mean free path of electrons passing through an electron gas of a density equal to that of Aluminum, as a function of the velocity, together with the double plasmon inverse mean free path of positrons (dashed line) and, also, the high-velocity limit of Eq. (2.24) multiplied by a factor of 2.16 (dotted line):

$$\lambda_{2p}^{-1} \approx 3.13 \times 10^{-3} \frac{\sqrt{r_s}}{v^2}. \quad (3.1)$$

At high velocities of the projectile the electron gas can be considered to be at rest, the effect of the Pauli restriction is, therefore, removed, and the behaviour of the double plasmon inverse mean free path, as a function of the velocity, is independent of the particle statistics. On the other hand, it is interesting to notice that the high-velocity limit of Eq. (3.1) gives

a good account of the full RPA result for both incident electrons and positrons in a wide range of projectile velocities. In particular, for Aluminum and an incident electron energy of 40keV we find from Eq. (3.1) a ratio for the double relative to the single plasmon of 1.93×10^{-3} , in agreement with the experiment¹⁶.

Contributions to the stopping power that are proportional to Z_1^2 and Z_1^3 , as obtained from Eqs. (2.29) and (2.34), are plotted in Fig. 5 by solid lines, as a function of the velocity, again for $r_s = 2.07$. It is interesting to notice that both Z_1^2 and Z_1^3 contributions to the stopping power exhibit a linear dependence on the velocity up to velocities approaching the stopping maximum; this linear dependence has, also, been observed for the low-velocity stopping power when it is calculated to all orders in the probe charge on the basis of density functional theory²³. The linear dependence of the Z_1^3 correction to the stopping power is, however, a consequence of two competing effects. First, there is the effect of one-step single excitations generated by the quadratically screened ion potential, represented by a dashed line in the same figure, and, then, the effect of two-step single excitations generated by the linearly screened ion potential, represented by a dashed-dotted line. The contribution from losses to two-step single excitations, represented by f_2 of Eq. (2.36), is very small, at high velocities, when the velocity distribution of target electrons can be neglected. In this case the static electron gas approximation can be made, the only non-vanishing contribution to the Z_1^3 effect comes, in this approximation, from f_1 of Eq. (2.35), i. e., from losses to one-step single excitations generated by the quadratically screened ion potential, and one finds that the result obtained in this approximation is well reproduced by Eq. (2.38), represented in Fig. 5 by a dotted line. This approximation gives a good account of the full RPA result, even at intermediate velocities where the velocity of target electrons is not negligible, and this is, again, a consequence of two competing effects. First, the non-negligible motion of the electron gas gives rise to a smaller contribution from losses to one-step single excitations, and this is almost compensated by the non-vanishing contribution from losses to two-step single excitations. Contributions from losses to double excitations are small in a wide range of projectile velocities and they are exactly equal to zero as far as the electron gas can be

considered to be at rest.

In order to analyze the contribution to the nonlinear stopping power coming from losses to collective excitations, we first show in Fig. 6 the separate contributions to the linear term from plasmon excitation and electron-hole pair excitation by the incident particle. For a momentum transfer that is smaller than q_c , the critical wave vector where the plasmon dispersion enters the electron-hole pair excitation spectrum, both the plasmon and the electron-hole pair excitation contribute to the energy loss, though contributions from losses from electron-hole pair excitations are very small. For $q > q_c$, however, only the excitation of electron-hole pairs contributes. Total contributions to the Z_1^2 stopping power coming from $q < q_c$ and $q > q_c$ are shown in Fig. 7, and contributions coming from $q < \sqrt{2\omega_p}$ and $q > \sqrt{2\omega_p}$ are plotted in Fig. 8, $\sqrt{2\omega_p}$ being the low-density limit of q_c . Contributions to the stopping power coming from losses to plasmons is, therefore, smaller than contributions from losses to electron-hole pairs, especially at high electron-densities, though there is, at high velocities, exact equipartition of the energy loss corresponding to momentum transfers larger than and smaller than $\sqrt{2\omega_p}$. This equipartition rule appears straightforwardly in the electron gas at rest approximation, and it has been formulated, for an electron gas not at rest, by Lindhard and Winther³⁴. This equipartition is, also, found to be exact, in the high velocity limit, by using Coulomb scattering of independent electrons with $q_{min} = \omega_p/v$ or by assuming that independent electrons are scattered by a velocity dependent Yukawa potential with screening length proportional to ω_p/v .

As far as the Z_1^3 stopping power is concerned, we have split the contributions to f_1 from losses to single plasmons and single electron-hole pairs, and we have found the result shown in Fig. 9 by dashed and dotted lines, respectively. On the other hand, all contributions to f_2 , represented in this figure by a dashed-dotted line, come from losses to electron-hole pairs. Thus, it is obvious from this figure that contributions to the Z_1^3 effect coming from losses to plasmons is small, showing that nonlinear corrections to losses from single plasmons are not important, and that collective excitations appear to be well described by linearly screened ion potentials. The equipartition rule, valid within first order perturbation theory and/or a

linear response theory of the electron gas, cannot be extended, therefore, to higher orders in the external perturbation.

Finally, in order to account approximately for the Z_1^3 effect coming from both the conduction band and the inner-shells, a local plasma approximation has been used, by assuming that a local Fermi energy can be attributed to each element of the solid, and experimental differences between the stopping power of silicon for protons and antiprotons have been successfully explained in this way²⁵.

IV. CONCLUSIONS

In conclusion, we have developed a quadratic response theory for the understanding of nonlinear aspects in the interaction of charged particles with matter. In the frame of many-body perturbation theory, we have studied the interaction of charged particles with the electron gas, within the random-phase-approximation, and in particular, the nonlinear wake potential generated by moving ions in matter, the Z_1^3 correction to the stopping power, and processes involved in multiple excitations of electron-hole pairs and plasmons.

Double plasmon mean free paths for incident electrons and positrons, and, also, second order contributions to the stopping power coming from the excitation of single and double plasmons have been evaluated, for the first time, in the full RPA, as a function of the velocity of the projectile.

Our results for the Z_1^3 correction to the stopping power show that for velocities smaller than the Fermi velocity the stopping power is, up to third order in the ion charge, a linear function of the projectile velocity. We have presented, for the high-velocity limit, a formula that gives a good account of the full RPA result in a wide range of projectile velocities, and our theory gives good agreement with the experiment. We have also separated the contributions to the stopping power coming from losses to plasmon generation, and we have found that collective excitations are well described by linearly screened ion potentials.

A nonlinear quantum hydrodynamical model of the electron gas has also been

developed³². It has been demonstrated that double plasmon excitation probabilities and the second order wake potential and stopping power coincide, within this model, with a plasmon-pole like approximation to our full RPA scheme, and an extension of this model to study the bounded electron gas is now in progress³⁵.

Full calculations of second order contributions to the wake potential and the induced electron density, within the RPA, for different values of the velocity of the projectile and the electron density of the medium will be published elsewhere³⁶.

An analysis of the differences between a self-energy approach to the Z_1^3 correction to the stopping power and the open diagrammatical approach presented here, and, also, investigations of the Z_1^3 stopping power for incident electrons and positrons are now in progress.

ACKNOWLEDGMENTS

The authors gratefully acknowledge discussions with P. M. Echenique and R. H. Ritchie. We wish also to acknowledge the support of the University of the Basque Country, the Basque Unibertsitate eta Ikerketa Saila, and the Spanish Comisión Asesora, Científica y Técnica (CAICYT).

REFERENCES

- ¹ P. M. Echenique, F. Flores, and R. H. Ritchie, in *Solid State Physics*, edited by E. H. Ehrenreich and D. Turbull (Academic, New York, 1990).
- ² D. Bohm and D. Pines, Phys. Rev. **92**, 609 (1953); D. Pines, Phys. Rev. **92**, 626 (1953).
- ³ J. Lindhard, K. Dan. Vidensk. Selsk. Mat.-Fys. Medd. **28**, no.8 (1954).
- ⁴ J. Hubbard, Proc. Phys. Soc. (London) **243**, 336 (1957).
- ⁵ K. S. Singwi, M. P. Tosi, R. H. Land, and A. Sjolander, Phys. Rev. **176**, 589 (1968); K. S. Singwi, A. Sjolander, M. P. Tosi, and R. H. Land, Phys. Rev. B **1**, 1044 (1970); K. S. Singwi and M. P. Tosi, Solid State Phys. **36**, 177 (1981).
- ⁶ S. L. Adler, Phys. Rev. **126**, 413 (1962); N. Wiser, Pys. Rev. **129**, 62 (1963).
- ⁷ O. H. Crawford and C. W. Nestor, Jr., Phys. Rev. A**28**, 1260 (1983).
- ⁸ N. D. Mermin, Phys. Rev. B **1**, 2362 (1970).
- ⁹ H. A. Bethe, Ann. Phys. (Leipzig) **5**, 325 (1930).
- ¹⁰ W. H. Barkas, W. Birnbaum, and F.M . Smith, Phys. Rev. **101**, 778 (1956); W. H. Barkas, N. J. Dyer, and H. H. Heckman, Phys. Rev. Lett. **11** 26 (1963); **11** 138(E) (1963).
- ¹¹ L. H. Andersen, P. Hvelplund, H. Knudsen, S.P. Moller, J. O. P. Pedersen, E. Uggerhoj, K. Elsener, and E. Morenzoni, Phys. Rev. Lett. **62**, 1731 (1989); R. Medenwalt, S. P. Moller, E. Uggerhoj, T. Worm, P. Hvelplund, H. Knudsen, K. Elsener, and E. Morenzoni, Nucl. Instrum. Methods **58**, 1 (1991); R. Medenwalt, S. P. Moller, E. Uggerhoj, T. Worm, P. Hvelplund, H. Knudsen, K. Elsener, and E. Morenzoni, Physics Letters A **155**, 155 (1991).
- ¹² J. C. Ashley, R. H. Ritchie, and W. Brandt, Phys. Rev. B **5**, 2393 (1972); **8**, 2402 (1973); **10**, 737 (1974).

- ¹³ C. C. Sung and R. H. Ritchie, Phys. Rev. A **28**, 674 (1983); C. D. Hu and E. Zaremba, Phys. Rev. B **37**, 9268 (1988); H. Mikkelsen and P. Sigmund, Phys Rev. A **40**, 101 (1989); H. Esbensen and P. Sigmund, Ann. Phys. **201**, 152 (1990).
- ¹⁴ J. M. Pitarke, R. H. Ritchie, and P. M. Echenique, Nucl. Instrum. Methods B **79**, 209 (1993); J. M. Pitarke, R. H. Ritchie, P. M. Echenique, and E. Zaremba, Europhys. Lett. **24**, 613 (1993).
- ¹⁵ J.C. Spence and A.E. Spargo, Phys. Rev. Lett. **26** 895 (1971).
- ¹⁶ P. Schattschneider, F. Fodermayr and D.S Su, Phys. Rev. Lett. **59**, 724 (1987).
- ¹⁷ J.C. Ashley and R.H. Ritchie, Phys. Stat. Sol. **38**, 425 (1970).
- ¹⁸ J. M. Pitarke and R. H. Ritchie, Nucl. Instrum. Methods B **90**, 358 (1994). Eq. (23) of this reference must be corrected and replaced by Eq. (10) of Ref. 19.
- ¹⁹ I. Campillo and J. M. Pitarke, Nucl Instrum. Methods B **115**, 75 (1996).
- ²⁰ A. Arnau and E. Zaremba, Nucl. Instrum. Methods B **90**, 32 (1994); J. J. Dorado, O. H. Crawford, and F. Flores, Nucl. Instrum. Methods B **93**, 175 (1994); erratum, Nucl. Instrum. Methods B (1994) (in press).
- ²¹ J. M. Pitarke, A. Bergara, and R. H. Ritchie, Nucl. Instrum. Methods B **99**, 87 (1995); A. Bergara and J. M. Pitarke, Nucl. Instrum. Methods B **96**, 604 (1995).
- ²² P. M. Echenique, R. M. Nieminen, and R. H. Ritchie, Solid State Commun. **37** 779 (1981); P. M. Echenique, R. M. Nieminen, J. C. Ashley, and R. H. Ritchie, Phys. Rev. A **33**, 897 (1986); J. C. Ashley, R. H. Ritchie, P. M. Echenique, and R. M. Nieminen, Nucl. Instrum. Methods B **15**, 11 (1986).
- ²³ E. Zaremba, A. Arnau, and P. M. Echenique, Nucl. Instrum. Methods B **96**, (1995).
- ²⁴ W. Brandt and M. Kitagawa, Phys. Rev. B **25**, 5631 (1982).

- ²⁵ J. M. Pitarke, R. H. Ritchie, and P. M. Echenique, Phys. Rev. B **52**, 13883 (1995).
- ²⁶ L. Hedin and S. Lundqvist, in *Solid State Physics*, edited by F. Seitz, D. Turbull, and E. H. Ehrenreich and (Academic, New York, 1990).
- ²⁷ J. J. Quinn and R. A. Ferrell, Phys. Rev. **112**, 812 (1958).
- ²⁸ R. H. Ritchie, Phys. Rev. **114**, 644 (1959).
- ²⁹ A. L. Fetter and J. D. Walecka, *Quantum Theory of Many-Particle Systems* (McGraw-Hill, New York, 1971).
- ³⁰ R. Cenni and P. Saracco, Nuclear Phys. A **487**, 279 (1988).
- ³¹ C. F. Richardson and N. W. Ashcroft, Phys. Rev. B **50**, 8170 (1994).
- ³² A. Bergara, J. M. Pitarke, and R. H. Ritchie, Nucl. Instrum. Methods B, **115**, 70 (1996).
- ³³ C. J. Tung and R. H. Ritchie, Phys. Rev. B **16**, 4302 (1977); J. C. Ashley, C. J. Tung, and R. H. Ritchie, Surf. Sci. **81**, 409 (1979); C. J. Tung, J. C. Ashley, and R. H. Ritchie, Surf. Sci. **81**, 427 (1979).
- ³⁴ J. Lindhard and A. Winther, K. Dan. Vidensk. Selsk. Mat.-Fys. Medd. **34**, no.4 (1964).
- ³⁵ A. Bergara, J. M. Pitarke, and F.J. García de Abajo, to be published.
- ³⁶ A. Bergara, I. Campillo, J. M. Pitarke, and P. M. Echenique, to be published.

FIGURES

FIG. 1. GW-RPA approximation to the self-energy.

FIG. 2. Diagrammatic representation, up to second order in the ion charge, of the RPA $S_{f_1 f_2, i_1 i_2}$ scattering amplitude. Solid internal lines in the first and second diagrams are zero-order propagators, and the triple internal vertex in the second diagram represents the quadratic density response function of the non-interacting electron gas. All vertex and self-energy insertions have been neglected, as well as ladder contributions.

FIG. 3. Diagrammatic representation of the matrix element of Eq. (2.26), as obtained within the RPA.

FIG. 4. Full RPA double plasmon inverse mean free path of electrons passing through an electron gas of a density equal to that of Aluminum ($r_s = 2.07$), as a function of the velocity (solid line). The dashed line represents the double plasmon inverse mean free path of positrons, and the dotted line, the high-velocity limit of Eq. (2.24).

FIG. 5. Full RPA Z_1^2 and Z_1^3 contributions to the stopping power calculated from Eqs. (2.29) and (2.34), respectively, for $Z_1 = 1$ and $r_s = 2.07$, as a function of the velocity of the projectile. Dashed and dashed-dotted lines represent Z_1^3 contributions from f_1 and f_2 of Eqs. (2.35) and (2.36), respectively. The dotted line represents the high-velocity limit of Eq. (2.38).

FIG. 6. Full RPA Z_1^2 contribution to the stopping power (solid line), versus velocity. Dashed and dotted lines represent contributions from plasmon and single electron-hole pair excitations, respectively.

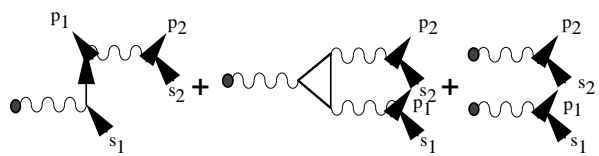
FIG. 7. Full RPA Z_1^2 contribution to the stopping power (solid line), versus velocity. Dashed and dotted lines represent total contributions for $q < q_c$ and $q > q_c$, respectively, q representing the momentum transfer, and q_c , the critical momentum for the plasmon being a well-defined excitation.

FIG. 8. As in Fig. 7, with q_c approximated by its low-density limit: $q_c = \sqrt{2\omega_p}$.

FIG. 9. Full RPA Z_1^3 contribution to the stopping power (solid line), as a function of the velocity of the projectile. The total contribution from f_1 of Eq. (2.35) (dashed line) has been split into contributions coming from losses to single plasmons (dashed-dotted-dotted-dotted line) and single electron-hole pairs (dotted line). The dashed-dotted line represents the total contribution from f_2 of Eq. (2.36), which appears as a consequence of losses to electron-hole pair excitations.

The diagram illustrates a perturbative expansion of a fermion propagator with a photon loop. On the left, a vertical solid line with an upward-pointing arrow represents the fermion. A wavy line (photon) forms a loop, with the momentum q labeled on the right and $p-q$ on the left. This is set equal to a sum of four terms:

- The first term is a vertical solid line with an upward-pointing arrow, with a dashed line forming a loop.
- The second term is a vertical solid line with an upward-pointing arrow, with a dashed line forming a loop and a solid circle (representing a fermion loop) attached to the right side.
- The third term is a vertical solid line with an upward-pointing arrow, with a dashed line forming a loop and two solid circles (representing fermion loops) attached to the right side.
- The fourth term is followed by an ellipsis \dots , indicating higher-order terms in the expansion.



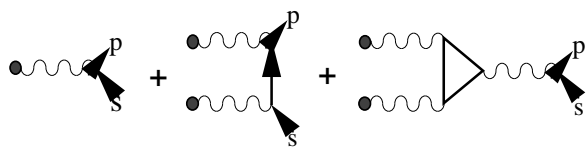


Fig. 4

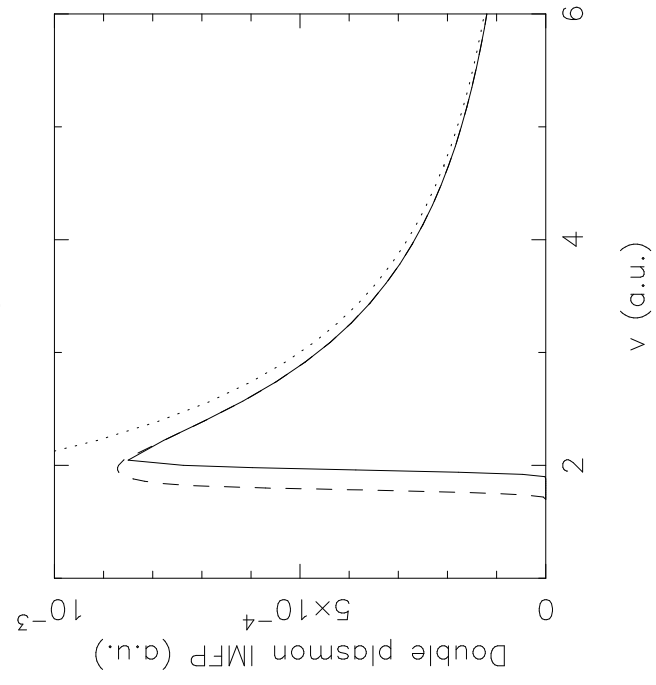


Fig. 5

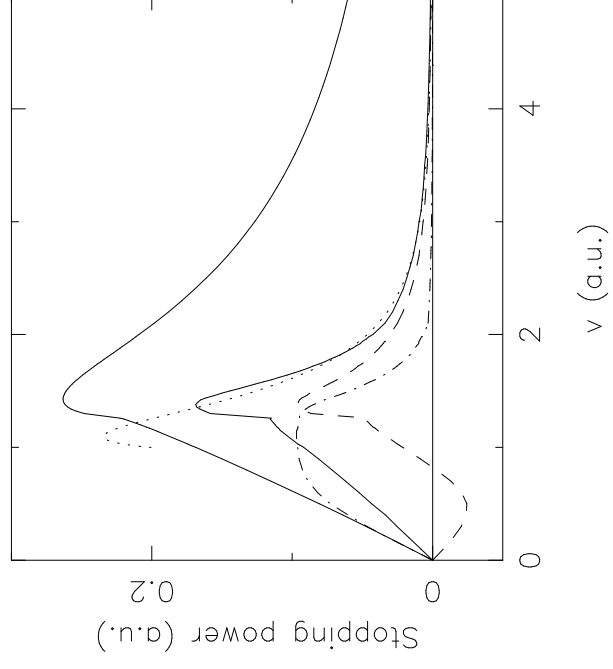


Fig. 6

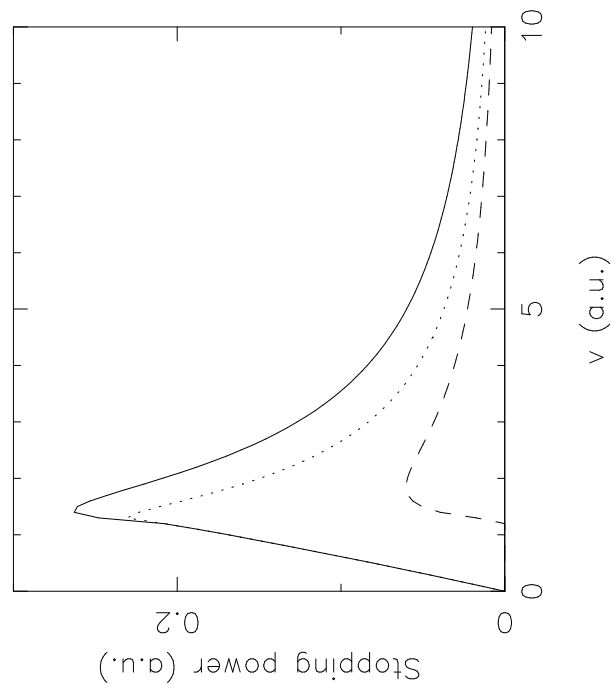


Fig. 7

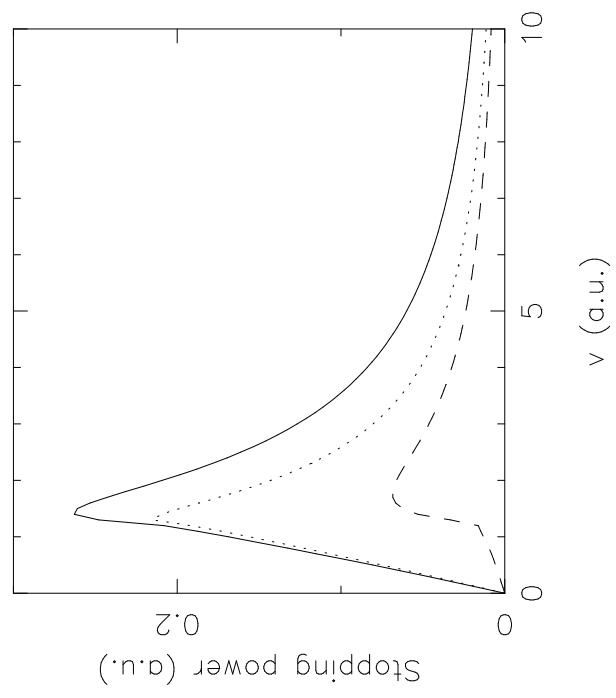


Fig. 8

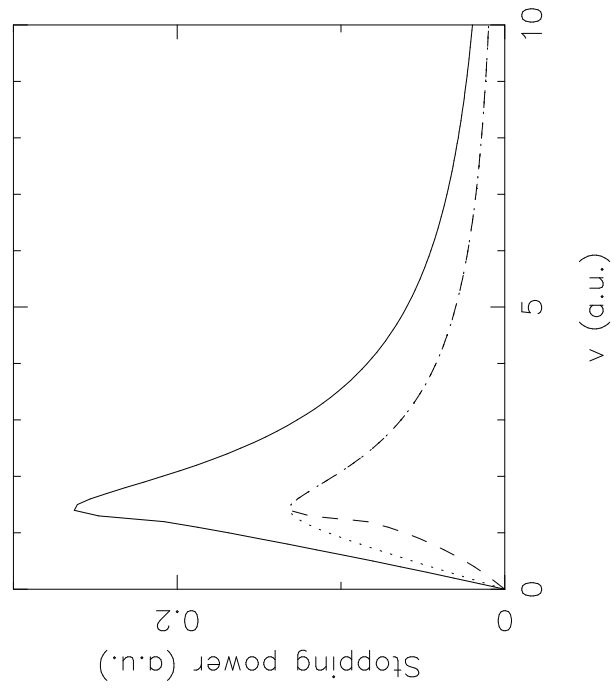


Fig. 9

